行政院國家科學委員會補助專題研究計畫成果報告

※※※※※※※※※※※※※※※※※※※※※※※※※
※ ※
※ **表面結構缺陷化學** ※
※ **Chemistry of Structural Defects on Surfaces** ※
※ ※
※※※※※※※※※※※※※※※※※※※※※※※※※

計畫類別：☑個別型計畫　□整合型計畫

計畫編號：NSC 89-2113-M-002-024

執行期間：88年8月1日至89年7月31日

計畫主持人：張哲政

共同主持人：

本成果報告包括以下應繳交之附件：

- □赴國外出差或研習心得報告一份 (N/A)
- □赴大陸地區出差或研習心得報告一份 (N/A)
- □出席國際學術會議心得報告及發表之論文各一份 (N/A)
- □國際合作研究計畫國外研究報告書一份 (N/A)

執行單位：臺灣大學化學系

中華民國89年12月25日

行政院國家科學委員會專題研究計畫成果報告

表面結構缺陷化學

Chemistry of Structural Defects on Surfaces

計畫編號： NSC 89-2113-M-002-024

執行期限： 88 年 8 月 1 日至 89 年 7 月 31 日

主持人： 張哲政

執行機構及單位：臺灣大學化學系

Abstract

Adsorption and decomposition of tert-butylacetylacetate (tBAA) on Si(100) have been investigated using static secondary ion mass spectrometry and temperature-programmed desorption. At low doses, all tBAA molecules dissociate readily upon adsorption on the surface at temperature as low as −160 ℃. The dissociation may occur through tBAA bonding via the ester oxygen or the carbonyl group to the surface. The bond scission occurring at the tBuO-CO bond leads to the formation of the surface tert-butoxide. Further dehydrogenation can take place to yield isobutene and surface hydroxyl species. Subsequent heating of the substrate causes the hydroxyl to decompose and the resulting substoichiometric silicon oxide sublimes as SiO. The surface-induced bond scission also occurs at the OC-CCO bond of the tBAA diketo moiety to produce isobutene. In addition, the OC-CCO bond scission induced by tBAA surface bonding mainly via its carboxylic keto oxygen affords acetaldehyde radical, whereas that mainly via the aceto oxygen yields carbon dioxide and isopropenoxy species. An enol-keto conversion takes place when isopropenoxy species acquire surface hydrogen to yield acetone, even at low substrate temperature of less than −126 ℃. The aceto oxygen pathway dominates the cleavage of the OC-CCO bond. Increasing substrate temperature also causes the surface tert-butyl fragments to further react through different β-hydride elimination pathways, forming isobutene, which is either in the gaseous state or bound to the surface in a di-σ configuration.

Key Words: chemical vapor deposition, β-diketonate complexes, static secondary ion mass spectrometry, β-hydride elimination, aceto oxygen pathway

Introduction

As mentioned in the original research proposal, the energetic ion beam has become increasingly popular during the last two decades for the characterization and modification of solids and surfaces. With this approach, the energy of the primary ion is typically in the range of several hundred eV to a few thousand eV. This energy is higher than the interaction energy normally present in chemical bonds. As a consequence, energetic ion beams offer a number of fascinating and novel challenges which promise to open new applications in materials/surface science. Our research effort has been directed toward a better understanding and utilization of the energetic ion probe. When a solid surface is bombarded with energetic ions, various processes take place in the surface region. Provided that these ions will not be reflected at the surface, they will penetrate to a certain depth into the solid and will transfer their energy to the lattice atoms. Further impacts distribute this energy to an extended lattice zone. A fraction of this energy reaches the surface again where it can induce the sputtering of surface atoms, ions, or clusters of atoms in a charged or uncharged state. Good understanding of the dynamics of the sputtering process has had a significant contribution to the development and growth of the microelectronic industry.

As the fabrication of the high-performance devices moves presently toward submicron dimensions, the chemical complexity involved in the formation of both the metastable and the final phases of materials and in the diagnostics of surface and interface properties of these phases is dramatically increased. Precise control of the energetic ion-beam-induced surface processes is thus a key issue for obtaining the desired

performance. In fact, when processed with the ion beam during the fabrication of devices, the substrate surface may reveal a substantial change of its chemical properties. Although ion-beam-induced chemical processes such as reactive-ion etching, focused-ion-beam assisted etching, and ion-beam assisted epitaxial deposition have been extensively utilized in the microelectronics industry for a variety of device applications, the fundamental nature that affects the alteration of the chemical reactivity of the bombarded surface has not been fully understood. It is well known that during the ion-beam process the material surface is extensively perturbed such that its electronic and structural properties are inevitably altered. The perturbation becomes more severe as the microelectronics industry moves toward nano-scale dimensions. For example, when the ion kinetic energy exceeds certain thresholds, such as that for bond disruption or surface penetration, disruption of the lattice by incident ions may create atomic-size aggregates and microstructures in the substrate. They may affect various surface material phenomena, such as dopant activation, alloy diffusion, and hillock growth, and artificial superlattice and eventually create a new pathway for surface chemical reaction. Under selected bombardment conditions, the ion-induced vacancies and defects from sputtering may also dominate the chemical behavior of the active layers and of the substrates of the nanostructural materials.

In order to obtain a better understanding of the chemical changes and the formation of these ion-induced structural defects in the solid surface due to sputtering, early studies were focused on the ion yield of different elements in relation to the compositional changes in the sputtered surface. The discovery of the anisotropy present in the angular distributions of particles ejected from the particle-bombarded single-crystal surfaces, however, brought the development of the sputter theory to a new territory. On the calculation side, the challenge is to be able to efficiently evaluate a large number of trajectories, each involving a few thousand atoms, such that the sputtering event can be modeled properly. A number of approaches to statistically extract information about the sputtering mechanistic process and the defect formation from this large volume of data have been utilized in the past, each yielding a certain degree of success. However, none of them are truly capable of providing the mechanistic information covering the entire energy and the angular domains in an efficient way.

In addition, there are also a few studies focused on the surface reaction of molecules containing an aceto group β to the keto group. Parmeter has used vibrational spectroscopy, thermal desorption measurements, and Auger spectroscopy to study the adsorption of hexafluoroacetylacetone (hfacH) on Pt(111).[37] His results indicated the formation of a "lying-down" hfacH. On Cu(111) and Cu(100),[38] however, only "standing-up" hfacH was formed, which did not begin to decompose until about 375 K. The adsorbed hfacH on these copper surfaces decomposed in a stepwise fashion to liberate fluorine, CO, CO_2, and fluorinated hydrocarbons. Furthermore, the interaction of hfacH on a stepped Cu(210) surface was reported to be fairly complete, with the formation of ten products desorbing in thirteen desorption states.[39]

Growing thin films by CVD using precursors containing β-diketonates thus exhibits perplexing chemistry. Since the growth kinetics and the microstructure of the films are determined by the molecular structure of the CVD precursor, fundamental studies of the interaction between tBAA and the silicon surface may thus serve to reveal surface intermediates that are involved in the overall deposition mechanism of bis(tert-butylacetoacetate)copper(II). Studies on tBAA surface decomposition can also demonstrate plausible mechanisms by which such ligand decomposition leads to impurity incorporation into the growing copper films. Since the chemistry of tBAA molecules as well as the chemistry of other ligands having a molecular structure of an ester group β to the carbonyl group are expected to be intimately related, the results obtained in this study are also of relevance to understanding the surface chemical mechanisms by which β-keto ester ligands fragment.

Experimental

All experiments are performed in a stainless steel ultrahigh vacuum chamber. The vacuum is maintained by a 220 L/s ion pump and a titanium sublimation pump, after the chamber is initially evacuated by sorption and turbomolecular pumps. A base pressure of 1×10^{-10} torr can be achieved after baking out, the residual gas being mostly hydrogen.

The working pressure is typically below 2.5 x 10^{-10} torr. This chamber is equipped with a quadrupole mass spectrometer (from Inficon), used for residual gas analysis and temperature-programmed desorption (TPD), another quadrupole mass spectrometer (from VG Microtech), used for static secondary ion mass spectrometry (SSIMS), a retarding field electron energy analyzer (from VG Microtech), used for both Auger electron spectroscopy (AES) and low-energy electron diffraction (LEED), and an ion gun (from VG Microtech). An electron impact ionizer is integrated to the Inficon mass spectrometer for detecting neutrals.

The Si(100) samples are acquired from International Wafer Service. They are antimony-doped (ρ = 0.0001 – 0.02 Ω-cm) and are cleaved into approximately 10 mm x 8 mm x 0.5 mm rectangles from wafers. Prior to being placed under the vacuum, the samples are subjected to a wet-chemical cleaning process,[40] including treatment of the surface with a HF solution for 1 min at room temperature followed by rinse with acetone and de-ionized water. This process produces a thin oxide layer that protects the underlayer silicon from further reaction. After the wet chemical treatment, two silicon samples are clipped together back to back, with a thin tantalum sheet sandwiched in between.[41] A pair of Chromel-Alumel thermocouples is spot-welded to the tantalum sheet for monitoring the sample temperature. For reference against the thermocouple, an optical pyrometer is used. The sandwiched silicon sample is then mounted to a manipulator using tantalum clamps. Once under ultrahigh vacuum, the protective oxide layer is removed by a slow annealing of 1-2 ℃/s to ~900 ℃, while maintaining the pressure below 3 x 10^{-9} torr, followed by a slow cooling to room temperature. In this work, sample heating up to 950 ℃ is obtained by passing a high electrical current through the sample, while cooling to –165 ℃ is made possible by conduction from a nearby copper tank filled with liquid nitrogen. The Si(100)-2x1 surface is then generated by repeated cycles of Ar ion sputtering (2 keV, 0.7 μA beam current, 1-2 x 10^{-6} torr, 30 min) and annealing (900 ℃, 2 min). Surface cleanness and perfection of the sample are checked by AES, LEED and SSIMS.

The tBAA is supplied by Acros and stored in a brown glass sample vial. It is further purified by several freeze-pump-thaw degassing cycles prior to dosing. The purity of the tBAA vapor is checked in situ by mass spectrometry. To admit the reactant tBAA into the vacuum system, a variable leak valve is used. The tBAA is introduced onto the sample through background exposure. All doses reported in this study are in langmuirs (1 L = 1 x 10^{-6} torr-s) of exposure at the sample surface. The exposure pressure is measured with an ionization gauge and is kept below 3 x 10^{-9} torr. The reading of the gauge is uncorrected for the corresponding sensitivity.

TPD experiments are conducted with the sample in line-of-sight of the mass spectrometer (non-differentially pumped). To preferentially admit gases desorbing directly from the sample surface to the ionizer, this spectrometer is fitted with a stainless skimmer with a 0.3 cm. diameter opening. For TPD measurements, the sample is placed ~0.1 in. away from the skimmer. Measurements of the intensities of desorbing species are controlled by interfacing the spectrometer control unit to a personal computer. During each TPD measurement, a linear temperature ramp is applied to the sample and the spectrometer is set to monitor several masses. A heating rate of 3 ℃/s is used in all TPD experiments.

SSIMS measurements are performed with the sample also in line-of-sight of the mass spectrometer (non-differentially pumped). A primary beam of Ar ions of 2 keV energy is used to bombard the sample, with the impact angle measured from the surface fixed at 45 degrees. The ion gun is differentially pumped and operated at a pressure of 3 x 10^{-9} torr when SSIMS spectra are recorded. With respect to the large cross section for sputter desorption and damaging, total ion currents are held within the 1-3 x 10^{-9} Amp range and the beam diameter is controlled to about 15 mm^2. A bias voltage of 22 V is applied to the sample to increase measured yield of secondary ions. Data collection is accomplished using an interface system designed by VG Microtech. The typical data collection time is <10 min/spectrum. No correction of the spectra for background is made.

Results and Discussion

Fig. 1 displays the SSIMS spectra taken by exposing a clean Si(100) sample to several different doses of tBAA. A typical SSIMS spectrum taken from a clean Si(100) surface shows peaks at m/e 28, 29, 30 and 56. The m/e peaks of 28, 29 and 30 result from the sputter desorption of Si^+ isotopes from the surface. The m/e 56 peak contains a

contribution from the sputter desorption of Si_2^+.

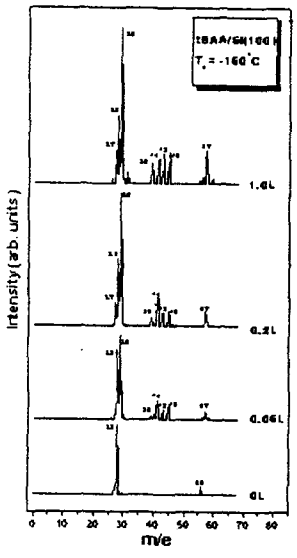

Figure 1. Secondary ion mass spectrum of a Si(100) surface exposed to the indicated doses of tBAA. A l spectra are recorded at –160 ℃. The spectra have been normalized to a constant peak height at m/e 28.

At low doses of less than 0.2 L, tBAA decomposes readily on the Si(100) sample even at low substrate temperature. As shown in Fig. 1, a number of m/e peaks at 28, 29, 41, 43, 45. and 57 can be identified in the SSIMS spectrum taken after the Si(100) surface is exposed to 0.06 L of tBAA at –160 ℃. No parent peak of tBAA (m/e 158) is observed in the spectrum. In fact, there is no noticeable signal present in the spectrum with m/e of higher than 57. According to the sputtering theory,[42] the secondary ions ejecting from the sample may originate from the positions located a few tens angstroms away from the point of impact where the ion-induced fragmentation of adsorbates may take place. Ion ejection from these far-away positions is brought about by momentum transferred late in the collision cascade from underneath atoms which move upward. These atoms usually have kinetic energies too low to cause dissociative emission of adsorbates.[43] Molecular ions of noticeable intensity may thus be detected when the current density and the total dose of the primary ion are minimized.[44] The absence of the tBAA molecular peak in Fig. 1 thus reveals that tBAA may all decompose on the Si(100) surface upon adsorption.

The decomposition of the low-dose tBAA on the sample surface is also supported by results from TPD experiments. In these experiments, an electron impact device is placed in front of the quadrupole mass analyzer for ionizing particles which thermally desorb from the sample surface. With the mass analyzer tuned in the tBAA molecular mass of 158, the TPD spectrum measured in the temperature range between –160 ℃ to 800 ℃ shows an absence of molecular signals for species desorbing from the Si(100) surface which has been exposed to 0.06 L of tBAA at –160 ℃. A test on the mass distribution of tBAA using the TPD detector reveals that the molecular signal, though small, can be detected when tBAA is deliberately introduced into the analysis chamber. Fig. 2 shows

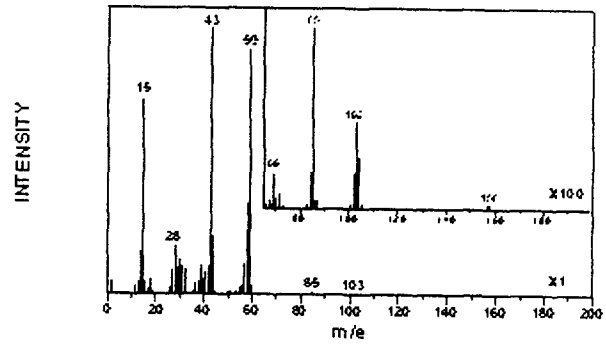

Figure 2. an electron-impact mass spectrum of tBAA.

an electron-impact mass spectrum obtained from a residual gas analysis (RGA) of the reaction chamber into which tBAA molecules of 1 x 10^{-8} torr partial pressure are deliberately introduced. This spectrum is constructed by subtracting the RGA mass spectrum measured after the tBAA introduction from the one obtained before the introduction. As shown in Fig. 2, when the reaction chamber contains tBAA molecules, a small peak intensity appears at m/e 158 in the mass spectrum, with a relatively large signal intensity observed at m/e 59. Assuming that the m/e 59 signal is an indication of the presence of tBAA molecules, a TPD study is then carried out by tuning the mass analyzer in m/e 59 to monitor if tBAA can desorb molecularly from the tBAA-dosed Si(100) surface when the substrate temperature is raised. Fig. 3 shows results from TPD experiments after the sample is exposed at –160 ℃ to tBAA of 0.06, 0.2, 1.0, and 3.0 L, respectively. As shown in the figure, no desorption signal can be identified in the m/e 59 spectrum when the tBAA exposure is less than 0.2 L. Coupling with the SSIMS results shown in Fig. 1, it appears that all tBAA molecules of low doses decompose readily upon adsorption on the Si(100) surface at –160 ℃. Comparing the fragment intensities with the m/e 28 intensity in the

SSIMS spectrum (Fig. 1), one can see that the surface concentration of the fragments from tBAA decomposition increases as the tBAA exposure is increased.

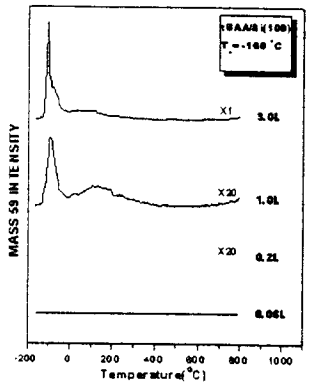

Figure 3. TPD Profiles for the m/e 59 species desorbing from Si(100) after various exposures of tBAA at -160 C.

The decomposition of all tBAA molecules of low exposure on the clean Si(100) surface at −160 ℃ is quite interesting, since as discussed in the introduction section many ester molecules can adsorb molecularly on the solid surface at low temperature.[31-36] The decomposition is not due to the ion-bombardment-induced fragmentation during SSIMS measurements, since a pilot SSIMS spectrum taken with data collection time of 30 seconds from the sample surface exposed to 0.06 L tBAA shows a similar intensity distribution as the one shown in Fig. 1, although the signal/noise ratio is poor. The absence of tBAA in the molecular state when adsorbed on the silicon surface at −160 ℃ may be accounted for in part by steric considerations. As an oxygenate, tBAA may bond to the sample surface via the ester group.[45] In addition, depending on the molecular orientation of tBAA relative to the surface at the time of adsorption, the diketo moiety of tBAA may also bond to the surface directly. In either bonding configuration, the surface would be active

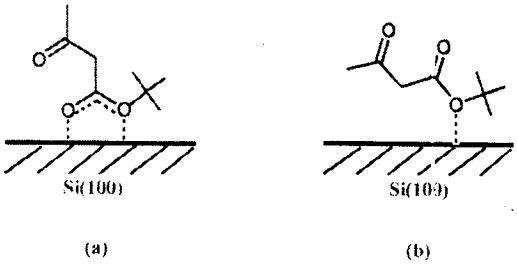

Figure 4. Illustration of possible initial states of adsorption of tBAA on Si(100).

for the rupture of chemical bonds. For tBAA to bond via the ester oxygen with (a η^3 configuration, Fig. 4a) or without (a η^1 configuration, Fig. 4b) the involvement of the ester carbonyl group, the surface may induce a bond scission at either the tBu-O bond or the tBuO-CO bond. The scission of the tBu-O bond produces tert-butyl fragment (m/e = 57) on the surface, which gives rise to the m/e 57 peak in the SSIMS spectrum (Fig. 1). It is known that bond cleavage is favored at the alkyl-substituted carbon atoms. The more a carbon atom is substituted, the more likely it is cleaved. The unique stability of tert-butyl fragments may thus facilitate the decomposition of tBAA molecules on the surface.

In addition, a bond cleavage at the tBuO-CO bond of tBAA may also be induced on the surface. The cleavage of the tBuO-CO bond may result in the formation of the tBuO-Si bond on the surface. The data obtained in this study does not shed light on the identity of the Si(100) adsorption site[46] to which tBuO prefers to bond, though synchrotron radiation photoemission study of ethanol on Si(100)[47] has ascertained a preferential dissociative chemisorption of ethanol on the surface dimers because of their distinct reactivity due to the buckled nature. It is also worth to note here that the preferred adsorption site can vary with the size of the alkyl group. Synchrotron radiation photoemission[48,49] and photostimulated desorption[49] studies of alcohol adsorption on Si(111) have shown that adsorption of the alkoxy species on the rest atoms becomes less favorable as the size of the alkyl group is increased.

Following the bond scission which occurs through binding of tBAA via the ester group, the surface reaction may proceed further. Two reaction products are most likely to be formed on the surface at −160 ℃. One product is isobutane, which is formed by attaching a surface hydrogen to the tert-butyl fragment. The major m/e peaks appearing in the reported electron-impact mass spectrum of isobutane usually include 43, 41, 42, 27, and 39 (in the order of a decreasing signal intensity[50]). The other product is isobutene, which may be formed by eliminating a hydrogen from the tert-butyl surface fragment or from the tBuO-Si surface species. Isobutene has a fragmentation pattern with the major m/e peaks in the electron-impact mass spectrum at 41, 39, 56, 28, 27 (in the order of a decreasing signal intensity[50]). Although the ionization process employed to obtain spectra shown in Fig. 1 is

different to the electron-impact process, the ratios of the integrated areas of the SSIMS peaks obtained following a 0.06 L dose of tBAA at −160 ℃ seem to be more consistent with the fragmentation pattern for isobutene.

The presence of isobutene on the surface due to tBAA decomposition upon adsorption s also supported by results from TPD experiments. Presented in Fig. 5 are TPD spectra taken with the

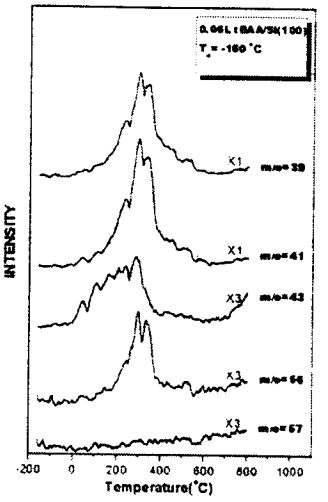

Figure 5 TPD profiles for a 0.06 L dose of tBAA on Si(100) at −160 ℃. The profiles are taken at indicated m/e and the heating rate is 3 ℃/s.

mass analyzer tuned in the indicated m/e values following a tBAA exposure of 0.06 L to S (100) at −160 ℃. The reaction products monitored in these TPD experiments include those with m/e = 39, 41, 43, 56 and 57. At 0.06 L tBAA exposure, m/e 56 is observed to desorb in the substrate temperature range between 150 and 400 ℃. In addition, the TPD profiles obtained at m/e 39 and 41 are in close resemblance to the one obtained at m/e 56, indicating that the m/e 39 and 41 species are fragments in the TPD ionizer of the one with m/e of 56. The ratios of the integrated areas of the TPD peaks, in which $Area_{41} > Area_{39} > Area_{56}$, is close to the reported ratios[50] of the signals in the electron-impact mass spectrum of isobutene. The resemblance of these TPD profiles and the similarity of the peak ratios to those of the reported spectrum confirm that isobutene (m/e = 56) is produced when tBAA molecules decompose on the Si(100) surface. It is noted that the electron-impact fragmentation pattern[50] for isobutane predicts an observation of the highest signal intensity in the mass spectrum from the m/e 43 fragment and the second highest from the m/e 41 fragment, if isobutane, instead of isobutene, was the major decomposition product of tBAA on the surface. Fig. 5, however, shows the opposite. The large difference in the m/e 41 and m/e 43 TPD profiles (shown in Fig. 5) also excludes the possibility that isobutane is the major product of the surface reaction which occurs following the surface-induced bond scission in the ester group of tBAA. Results of this study, however, cannot leave out the possibility that small amounts of isobutane may also be produced from the surface decomposition of tBAA.

There are two different groups of surface reaction pathways that may account for the observed production of isobutene. One is via elimination of a hydrogen from the surface alkyl fragment, the other from the alkoxy species. The elimination of hydrogen from the alkyl species on the surface to yield alkene has been reported in the literature. Studies using high-resolution electron energy loss spectroscopy and x-ray photoelectron spectroscopy about the adsorption chemistry of tertiarybutylphosphine on Si(100) have shown that tertiarybutylphosphine can be partially decomposed on the surface at room temperature.[51] Increasing the substrate temperature would then cause butene to evolve, with a broad m/e 56 peak in the TPD spectrum between 100 and 400 ℃. No TPD peaks were found for the $C_4H_9^+$ spectrum (m/e = 57) up to 650 ℃. The peak temperature range for m/e 56 and the absence of the m/e 57 peak are in consistent with our observations (Fig. 5). Based on Fourtier transform infrared-attenuated total reflection (FTIR-ATR) and TPD studies of the reaction of tert-butyl silane on Si(100), E. Rudkevich et al. also concluded the presence of isobutene on the surface, after bond cleavage first took place at the Si-C bond to form tert-butyl species.[52] These reports reveal that the production of alkene on the Si(100) surface does not have to go through the alkoxy reaction pathway, since in either case no surface alkoxy intermediates can be generated.

*** The results of this study have been accepted for publication in Journal of Physical Chemistry.**

Refeences

1. J. E. Parmeter, J. Phys. Chem. 97 (1993) 1530.

2. G. S. Girolami, P. M. Jeffries, L. H. Dubois, J. Am. Chem. Soc. 115 (1993) 1015.

3. H. L. Nigg, R. I. Masel, Surface Sci. 409 (1998) 428.

4. A. Ishizaka, Y. Shiraki, J. Electrochem. Soc. 133 (1985) 666.

5. F. Bozso, J. T. Yates, Jr., W. J. Choyke, L. Muehlhoff, J. Appl. Phys. 57 (1985) 2771.

6. C.-C. Chang, J.-Y. Hsieh, Phys. Rev. B57 (1998) 57.

7. B. J. Garrison, J. Am. Chem. Soc. 102 (1980) 6553.

8. A. L. Schwaner, J. E. Fieberg, J. M. White, J. Phys. Chem. B101 (1997) 11112.

9. A. L. Schwaner, J. M. White, J. Phys. Chem. B101 (1997) 11119.

10. E. Zahidi, M. Castonguay, P. H. McBreen, J. Am. Chem. Soc. 116 (1994) 5847.

11. B. A. Sexton, A. E. Hughes, N. R. Avery, Surf. Sci. 155 (1985) 366.

12. B. A. Sexton, A. E. Hughes, N. R. Avery, Appl. Surf. Sci. 22/23 (1985) 404.

13. S. D. Worley, J. T. Yates, Jr. J. Catal. 48 (1977) 395.

14. M. M. Walczak, P. K. Leavitt, P. A. Thiel, J. Am. Chem. Soc. 109 (1987) 5621.

15. T. Hashizume, R. J. Hamers, J. E. Demuth, K. Markert. T. Sakurai, J. Vac. Sci. Technol. A8 (1990) 249.

16. M. P. Casaletto, R. Zanoni, M. Carbone, M. N. Piancastelli, L. Aballe, K. Weiss, K. Horn, Surf. Sci. 447 (2000) 237.

17. M. Carbone, M. N. Piancastelli, J. J. Paggel, Chr. Weindel, K. Horn, Surf. Sci. 412/413 (1998) 441.

18. M. Carbone, R. Zanoni, M. N. Piancastelli, G. Comtet, G. Dujardin, L. Hellner, Surf. Sci. 352-354 (1996) 391.

19. E. Stenhagen, S. Abrahamsson, F. W. McLafferty, "Atlas of Mass Spectral Data", eds., Interscience Publishers, New York

20. G. Kaneda, J. Murata, T. Takeuchi, Y Suzuki, N. Sanada, Y. Fukuda, Appl. Surf. Sci. 113/114 (1997) 546.

21. E. Rudkevich, D. Saulys, D. Gains, T. F. Kuech, L. McCaughan, Surf. Sci. 383 (1997) 69.